Article

In Vitro and *in Vivo* Evaluation of Doxorubicin Conjugates with the Divalent Peptide E-[c(RGDfK)] that Targets Integrin

Claudia Ryppa, Hagit Mann-Steinberg, Iduna Fichtner, Holger Weber, Ronit Satchi-Fainaro, Martin L. Biniossek, and Felix Kratz

Bioconjugate Chem., **2008**, 19 (7), 1414-1422 • DOI: 10.1021/bc800117r • Publication Date (Web): 26 June 2008

In Vitro and *in Vivo* Evaluation of Doxorubicin Conjugates with the Divalent Peptide E-[c(RGDfK)$_2$] that Targets Integrin $\alpha_v\beta_3$

Claudia Ryppa,[†] Hagit Mann-Steinberg,[‡] Iduna Fichtner,[§] Holger Weber,[||] Ronit Satchi-Fainaro,[‡] Martin L. Biniossek,[⊥] and Felix Kratz*,[†]

Tumor Biology Center, Breisacher Straβe 117, 79106 Freiburg, Federal Republic of Germany, Department of Physiology and Pharmacology, Sackler School of Medicine, Tel-Aviv University, Tel-Aviv 69978, Israel, Max-Delbrück Center, Robert-Rössle-Straβe 10, 13122 Berlin, ProQinase, Breisacher Straβe 117, 79106 Freiburg, and Institut für Molekulare Medizin and Zellforschung, Zentrum für Biochemie and Molekulare Zellforschung, Stefan-Meier-Straβe 17, 79104 Freiburg, Federal Republic of Germany. Received March 20, 2008; Revised Manuscript Received May 15, 2008

Integrins, especially integrin $\alpha_v\beta_3$, are attractive receptors for vascular targeting strategies. Recently, a divalent RGD peptidomimetic, E-[c(RGDfK)$_2$], has been described that demonstrates increased uptake in human ovarian carcinoma OVCAR-3 xenograft tumors. Inspired by these results, we set out to develop doxorubicin conjugates with E-[c(RGDfK)$_2$] by binding two different maleimide derivatives of doxorubicin to E-[c(RGDfK)$_2$] that was thiolated with iminothiolane. In this way, two water-soluble derivatives were obtained, E-[c(RGDfK)$_2$]-DOXO-1 and E-[c(RGDfK)$_2$]-DOXO-2. In E-[c(RGDfK)$_2$]-DOXO-1, doxorubicin was bound to the peptide through a stable amide bond, and in E-[c(RGDfK)$_2$]-DOXO-2, a MMP-2/MMP-9 cleavable octapeptide was introduced between doxorubicin and the peptide. The rationale for a MMP-2/MMP-9-cleavable linker was that MMP-2 and MMP-9 bind to integrin $\alpha_v\beta_3$ and both are overexpressed in tumor vasculature. In addition, analogous control doxorubicin-containing peptides bearing c(RADfK) that does not bind to integrin $\alpha_v\beta_3$ were synthesized, i.e., c(RADfK)-DOXO-1 and c(RADfK)-DOXO-2. Whereas E-[c(RGDfK)$_2$]-DOXO-2 was cleaved effectively by MMP-2 and in OVCAR-3 tumor homogenates releasing a doxorubicin-tetrapeptide or doxorubicin as the final cleavage product, no release of doxorubicin was observed for E-[c(RGDfK)$_2$]-DOXO-1. Proliferation of HUVEC in the presence of MMP-2-cleavable doxorubicin-containing peptides exhibited 6- to 10-fold increased inhibition compared to the amide-linked doxorubicin-containing peptides. In addition, inhibition of HUVEC sprouting during a 24 h exposure was approximately 3-fold stronger for E-[c(RGDfK)$_2$]-DOXO-2 and 20-fold stronger for the reference peptide conjugate c(RADfK)-DOXO-2 than for doxorubicin alone. *In vivo* studies in an OVCAR-3 xenograft model demonstrated no or only moderate antitumor efficacy for either E-[c(RGDfK)$_2$], E-[c(RGDfK)$_2$]-DOXO-1, E-[c(RGDfK)$_2$]-DOXO-2, or c(RADfK)-DOXO-2, even at doses of 3 × 24 mg/kg doxorubicin equivalents, compared to an improved antitumor effect for doxorubicin at 2 × 8 mg/kg.

INTRODUCTION

Vascular targeting agents interact with receptors on endothelial cells and, unlike antiangiogenic drugs that inhibit the formation of new vessels, destroy or occlude pre-existing blood vessels of solid tumors (*1*). Vascular targeting agents can act as inhibitors of endothelial growth such as combretastatins or receptor antagonists or they comprise ligand-based drugs consisting of a targeting moiety and an effector molecule. Suitable receptors on endothelial cells for ligand-directed approaches are the VEGF[1] receptors, the fibronectin ED-B domain, endoglin, NG2 proteoglycan, prostate-specific membrane antigen (PSMA), as well as cell adhesion receptors such as vascular cell adhesion molecule 1 (VCAM-1), E-selectins, and integrins (*1–4*). The latter have perhaps been the most intensely studied as endothelial targets for vascular targeting agents (*5*). Integrins are heterodimeric cell surface receptors of which several such as integrin $\alpha_v\beta_3$, $\alpha_v\beta_5$, and $\alpha_5\beta_1$ are overexpressed in the blood vessels of solid tumors and mediate adhesion between cells and the extracellular matrix, thus promoting tumor cell migration and tumor growth (*3*). A characteristic feature of integrins is their high binding affinity for arginyl-glycyl-aspartic acid (RGD) sequences exposed on endogenous or exogenous ligands. Using an *in vivo* phage display technology, Arap and co-workers discovered cyclic RGD-4C peptides that bind avidly to integrin $\alpha_v\beta_3$ and $\alpha_v\beta_5$ (*6, 7*). A number of doxorubicin conjugates have been developed with a divalent RGD-4C peptide (ACDCRGDCFCG). The first by Arap et al. who coupled the 3′-amino position of doxorubicin to one or two of the free carboxylate groups of RGD-4C by activating the latter with 1-ethyl-3-(3,3-dimethylaminopropyl)carbodiimide and *N*-hydroxysuccinimide. This conjugate showed improved activity and toxicity profile over doxorubicin in a MDA-MB-435 mammary carcinoma model

* To whom correspondence should be addressed. Dr. Felix Kratz, Tumor Biology Center, Department of Medical Oncology, Clinical Research, Breisacher Straβe 117, D-79106 Freiburg, Federal Republic of Germany. Tel.: 0049-761-2062930. Fax: 0049-761-2062905. E-mail: felix@tumorbio.uni-freiburg.de.

[†] Tumor Biology Center.

[‡] Tel-Aviv University.

[§] Max-Delbrück Center.

[||] ProQinase.

[⊥] Institut für Molekulare Medizin and Zellforschung.

[1] Abbreviations: VEGF, vascular endothelial growth factor; OVCAR, ovarian carcinoma; MMP, matrix metalloprotease; HUVEC, human umbilical vein endothelial cells; AcN, acetonitrile; TFA, trifluoroacetic acid; EX, excitation; EM, emission; TOF, time of flight; APMA, *p*-aminophenylmercuric acetate; Tris, Tris-(hydroxymethyl)-aminomethane; EBM-2, endothelial cell basal medium 2; EGM-2, endothelial growth medium 2; FBS, fetal bovine serum; EC, endothelial cells; nu/nu, Nude; i.v., intravenous; s.c., subcutaneous; i.p., intraperitoneal; ID/g, injected doses/gram; MTD, maximum tolerated dose; T/C, tumor volume test/control; BWC, body weight change.

10.1021/bc800117r CCC: $40.75
Published on Web 06/26/2008

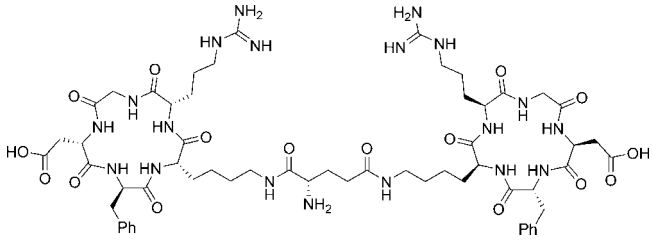

Figure 1. Structure of E-[c(RGDfK)$_2$].

in which integrin $\alpha_v\beta_3$ is expressed in the tumor vessels as well as on the tumor cell themselves (*7, 8*). Superior efficacy of the RGD-4C-doxorubicin conjugate was confirmed in another model (hepatoma) in which the tumor cells did not express integrin $\alpha_v\beta_3$ suggesting that a direct endothelial effect was responsible for tumor growth inhibition (*8*). The precise structure and mode of action of these conjugates has not been reported, but conjugation at the 3′-amino group seems likely resulting in a stable amide bond between doxorubicin and the divalent peptide which presumably cannot be readily cleaved *in vivo*. This led de Groot et al. to develop a prodrug with RGD-4C and a plasmin-cleavable substrate D-Ala-Phe-Lys that showed comparable *in vitro* cytotoxicity to doxorubicin after activation by plasmin (*9*). Unfortunately, no *in vivo* efficacy has been reported for this conjugate. Due to the presence of two disulfide bridges in the structure of RGD-4C that are prone to cleavage during synthesis or in biological media, a stable peptide derivative E-[c(RGDfK)$_2$] based on the integrin $\alpha_v\beta_3$ antagonist Cilengitide has been developed that shows specific tumor targeting properties (*10–13*). The presence of the glutamic acid residue makes it an ideal ligand for further chemical conjugation. Burkhart et al. conjugated a doxorubicin prodrug, doxsaliform, to this position and showed that the resulting conjugate bound specifically to vitronectin and that *N*-methylhydroxyl-doxorubicin is released by hydrolysis as the highly cytotoxic doxorubicin derivative, but no *in vivo* data were reported (*14*).

Further diagnostic studies by Janssen et al. demonstrated that a dimeric form of c(RGDfK) (Figure 1), i.e. E-[c(RGDfK)$_2$], has improved tumor targeting properties over the monomeric form (*12, 14*). Subsequent biodistribution studies with radiolabeled E-[c(RGDfK)$_2$] showed an uptake of up to 7.5% injected dose/g in OVCAR-3 xenograft tumors (*12*).

Inspired by these results, we set out to develop doxorubicin conjugates with E-[c(RGDfK)$_2$]. Our aim was to (a) develop a stable drug derivative as well as a prodrug with RGD peptides, (b) to establish the *in vitro* properties of these drug conjugates including analogously constructed conjugates with the nonintegrin $\alpha_v\beta_3$ binding control peptide c(RADfK), and (c) to compare the *in vivo* efficacy of the RGD doxorubicin conjugates in the human ovarian carcinoma OVCAR-3 xenograft model which was used by Janssen et al. for biodistribution studies with E-[c(RGDfK)$_2$], in the hope of answering some of the open questions regarding cleavability and *in vivo* potential that have arisen in this particular area of doxorubicin conjugates.

As starting materials for the intended doxorubicin RGD-based peptide conjugates, we used the 6-maleimidocaproyl amide derivative of doxorubicin **1** as a stable derivative and the maleimidotriethylene glycol peptide derivative **2** that contains an octapeptide that is cleaved by matrix metalloproteases 2 and 9 (MMP-2 and MMP-9) (Figure 2). A MMP-2/-9 cleavable prodrug seemed suitable for our vascular targeting strategy considering that MMP-2 and MMP-9 bind to integrin $\alpha_v\beta_3$ and both are overexpressed in tumor vasculature (*15–17*) which could ensure that sufficient amounts of these proteases are present at the molecular target after binding of the doxorubicin RGD peptides to integrin $\alpha_v\beta_3$. In addition, compound **2**, developed as an albumin binding prodrug, demonstrated superior *in vivo* efficacy compared to doxorubicin in a melanoma xenograft model (*18*).

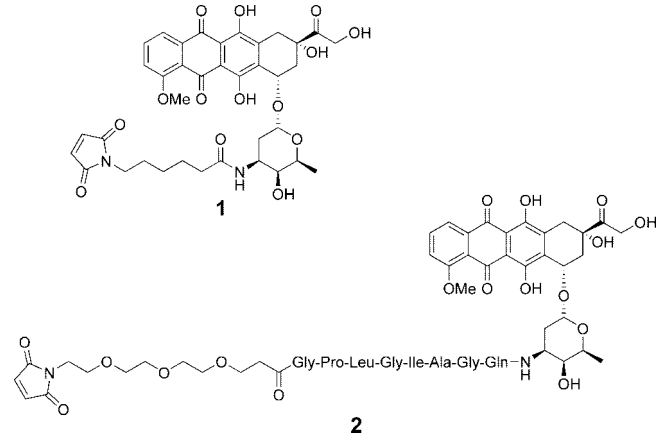

Figure 2. Stable 6-maleimidocaproyl amide derivative of doxorubicin **1** and the MMP-2 cleavable maleimidotriethylene glycol peptide derivative **2**.

EXPERIMENTAL PROCEDURES

Materials and Instrumental. Doxorubicin hydrochloride was purchased from Yick-Vic (Hong Kong, PRC); E-[c(RGDfK)$_2$] and c(RADfK) were purchased from Peptides International (Louisville, KY, USA); organic solvents: HPLC grade (Labscan Ltd., Dublin, Ireland; Roth, Karlsruhe, FRG; Merck, Darmstadt, FRG). Compound **2** was prepared as described in the literature (*18*). All other chemicals used were at least reagent grade and obtained from Sigma-Aldrich (Deisenhofen, FRG), Roth, or Merck and used without further purification; buffers were vacuum-filtered through a 0.2 μm membrane (Sartorius, Göttingen, FRG) and thoroughly degassed with nitrogen prior to use. ^{1}H, ^{13}C NMR: Bruker AM 400 (internal standard: TMS); analytical HPLC were performed with a Kontron 422 pump and a Kontron 430 detector (at 495 and 254 nm). For peak integration, *Geminyx* software (v 1.91 by Goebel Instrumentelle Analytik, FRG) was used; column: Machery-Nagel, 100 Å, Nucleosil 100−5 C18 [4 × 250 mm] with precolumn; chromatographic conditions: flow: 1.0 mL/min, mobile phase A: AcN/0.05% aq. TFA (30/70, v/v), mobile phase B: AcN/0.05% aq. TFA (70/30, v/v), gradient: 0−1.5 min 100% mobile phase A; 1.5−40 min increase to mobile phase B; 40−46.5 min decrease to initial mobile phase A; injection volume: 20 μL. Cleavage studies with MMP-2 and in OVCAR-3 tumor homogenates were performed following a modified method according to the literature (*18*) with a Kontron 422 pump and a Merck F-1050 fluorescence spectrophotometer (EX 490 nm, EM 540 nm). For peak integration, *Geminyx* software was used; column: Waters WAT106151, Symmetry 300, C18 5 μ [4.6 × 250 mm] with precolumn WAT106166; chromatographic conditions: flow: 1.0 mL/min, mobile phase A: AcN/0.05% aq. TFA (25/75, v/v), mobile phase B: AcN/0.05% aq. TFA (55/45, v/v), gradient: 0−25 min 100% mobile phase A; 25−40 min increase to mobile phase B; 40−50 min 100% mobile phase B; 50−60 min decrease to initial mobile phase A; injection volume: 20 μL. Preparative HPLC for the separation of E-[c(RGDfK)$_2$]-DOXO-1, E-[c(RGDfK)$_2$]-DOXO-2, c(RADfK)-DOXO-1, and c(RADfK)-DOXO-2 was performed with a BioLogic Duo-Flow System from Biorad (München, FRG) which was connected with a Lambda 1010 visible monitor from Bischoff (at λ = 495 nm); UV-detection at λ = 254 nm from Biorad; column: Machery-Nagel, 100 Å, Nucleosil 100−7 C18 [21 × 250 mm] with precolumn; chromatographic conditions: flow: 10 mL/min,

mobile phase A: AcN/0.05% aq. TFA (30/70, v/v), mobile phase B: AcN/0.05% aq. TFA (70/30, v/v), gradient: 0−1 min 100% mobile phase A; 1−44 min increase to mobile phase B; 41−46 min decrease to initial mobile phase A; injection volume: 2 mL. MALDI-TOF mass spectra were acquired on a Reflex III mass spectrometer (Bruker Daltonik GmbH, Bremen, FRG) in the reflector mode (positively charged ions) with external calibration. Samples were prepared with an adapted thin-layer technique (*19*). α-Cyano-4-hydroxycinnamic acid (97%, Aldrich, Taufkirchen, FRG) was used as matrix and nitrocellulose (Biorad, Trans-Blot Transfer Medium) as additive. The samples were washed with 0.1% TFA. Monoisotopic peaks were used for data analysis. ESI-TOF mass spectra were acquired on an Agilent 6210 system, consisting of an Agilent 1100 HPLC system with a diode array detector and an ESI-MSD TOF by Agilent Technologies (Böblingen, FRG).

Synthesis of 6-Maleimidocaproylamide Derivate of Doxorubicin 1. Doxorubicin hydrochloride (500 mg, 0.86 mmol, 1 equiv), 6-maleimidocaproylic acid *N*-hydroxysuccinimide ester (292 mg, 0.95 mmol, 1.1 equiv), and triethyl amine (239 μL, 1.74 mmol, 2 equiv) were dissolved in DMF (30 mL) and stirred for 2 h at room temperature. The solution was precipitated in diethyl ether (10 mL), washed with dry diethyl ether (2 × 5 mL), filtered and dried *in vacuo* to obtain red crystals in 91% yield (574 mg, 0.78 mmol); HPLC analysis: 14.4 min, 96% of peak area, 495 nm; MS (ESI-TOF) m/z = 775.21 $[M + K]^+$, 759.24 $[M + Na]^+$.

General Procedure for the Synthesis of E-[c(RGDfK)$_2$]-DOXO-1, E-[c(RGDfK)$_2$]-DOXO-2, c(RADfK)-DOXO-1, and c(RADfK)-DOXO-2. The doxorubicin derivatives **1** (20 mM solution in DMF) or **2** (1 equiv) and E-[c(RGDfK)$_2$] or c(RADfK) (1 equiv) were dissolved in 10 mM sodium phosphate buffer (8−20 mL, containing 1 mM EDTA, pH 7.5). A 72.7 mM solution of 2-iminothiolane (1 equiv) in 10 mM sodium phosphate buffer (containing 1 mM EDTA, pH 7.5) was added to the clear red solution and the mixture was kept overnight at room temperature. The solvent was removed *in vacuo*; the residue was dissolved in 2 mL AcN/0.05% aq. TFA (30/70, v/v) and purified by preparative HPLC.

E-[c(RGDfK)$_2$]-DOXO-1. Red crystals were obtained in 44% yield (42 mg, 0.017 mmol). HPLC analysis: 10.3 min, >97% of peak area, 495 nm; MS (TOF) m/z = 2177.90 $[M + Na]^+$, 2155.93 $[M + H]^+$, 1759.84 $[C_{79}H_{119}N_{22}O_{22}S]^+$.

E-[c(RGDfK)$_2$]-DOXO-2. Red crystals were obtained in 62% yield (60 mg, 0.018 mmol). HPLC analysis: 12.1 min, 95% of peak area, 495 nm; MS (TOF) m/z = 2939.35 $[M + H]^+$, 2543.27 $[C_{113}H_{176}N_{31}O_{34}S]^+$.

c(RADfK)-DOXO-1. Red crystals were obtained in 29% yield (43 mg, 0.026 mmol). HPLC analysis: 11.3 min of peak area, 95%, 495 nm; MS (TOF) m/z = 1455.61 $[M + H]^+$, 1059.55 $[C_{48}H_{75}N_{12}O_{13}S]^+$.

c(RADfK)-DOXO-2. Red crystals were obtained in 43% yield (81 mg, 0.033 mmol). HPLC analysis: 12.9 min, 91% of peak area, 495 nm; MS (TOF) m/z = 2261.04 $[M + Na]^+$, 2239.06 $[M + H]^+$, 1842.97 $[C_{82}H_{132}N_{21}O_{25}S]^+$.

Cleavage Studies of E-[c(RGDfK)$_2$]-DOXO-2 with 58.8 mU/μL Activated MMP-2. A 200 μM solution of E-[c(RGDfK)$_2$]-DOXO-2 in 50 mM Tris·HCl buffer (pH 7.5) was prepared. A 10 mM stock solution of *p*-aminophenylmercuric acetate (APMA, 3.9 mg) in 0.1 M NaOH (1 mL) was diluted with 50 mM Tris·HCl buffer (3 mL, pH 7.5) to obtain a 2.5 mM APMA solution which was adjusted to pH 7.2. MMP-2 (58.8 mU) was activated for 30 min at 37 °C with 7.5 μL of the 2.5 mM APMA solution. 100 μL of the E-[c(RGDfK)$_2$]-DOXO-2 stock solution (200 μM) were mixed with activated MMP-2 and incubated at 37 °C. Samples were collected and analyzed by HPLC over 3 h.

Cleavage Studies of E-[c(RGDfK)$_2$]-DOXO-2 with OVCAR-3 Tumor Homogenates. For preparing the tumor homogenates, tissues of OVCAR-3 xenografts were cut into small pieces, and 200 mg samples were transferred in a 2 mL Eppendorf tube to which was added 800 μL of buffer (50 mM Tris·HCl buffer, pH 7.4, containing 1 mM monothioglycerol). Homogenization was carried out with a microdissmembrator at 2000 rpm for 2 × 10 min with the aid of glass balls. Subsequently, the samples were centrifuged at 10 000 rpm for 10 min at 4 °C. The supernatant was aliquoted and kept frozen at −78 °C prior to use.

100 μL of the E-[c(RGDfK)$_2$]-DOXO-2 stock solution (200 μM) were mixed with OVCAR-3 tumor homogenate at pH 7.4 and incubated at 37 °C. Samples were collected and analyzed by HPLC over 75 min.

Endothelial Cell Proliferation Assay. HUVEC were plated onto 24-well plate (1.5 × 10^4 cells/well) in EBM-2 medium (Clonetics, Walkersville, MD, USA) supplemented with 5% FBS and incubated for 24 h (37 °C; 5% CO_2). On the following day, the cultured medium was removed and cells were exposed to serial dilutions of doxorubicin derivatives prepared in a fresh mixture of EBM-2 medium and EGM-2 complete medium (Clonetics) (1:1, v/v). Cell proliferation was assessed after 72 h by means of direct counting using a Z1 Coulter Particle Counter (Beckman Coulter, Luton, England). As positive control, cells were grown without treatment. Each treatment was assayed in triplicates and the experiment was repeated independently. Proliferation of endothelial cells was normalized to percent cell growth compared to the cell growth of the positive untreated control cells. Error bars represent the standard deviation of the mean.

Endothelial Cell Sprouting Assay. HUVEC were purchased from PromoCell (Heidelberg, FRG) and used at passage 3−4. The experiments were pursued in modification of the originally published protocol (*20, 21*). In brief, spheroids were prepared as described by pipetting 500 endothelial cells (EC) in a hanging drop on plastic dishes to allow overnight spheroid aggregation. 50 EC spheroids were then seeded in 0.9 mL of a collagen solution and pipetted into individual wells of a 24 well plate to allow polymerization. The test compounds were added after 30 min by pipetting 100 μL of a 10-fold concentrated working dilution on top of the polymerized gel in combination with VEGF-A (25 ng/mL, ProQinase, Freiburg, FRG). Plates were incubated at 37 °C for 24 h and fixed by adding 4% paraformaldehyde. Sprouting intensity of EC spheroids was quantitatively determined by the cumulative sprout length per spheroid using an inverted microscope and the digital imaging software *Analysis 3.2* from Soft Imaging System (Münster, FRG). The mean of the cumulative sprout length of 10 randomly selected spheroids was analyzed as an individual data point and the relative inhibition by the test compounds determined. Fitting of IC_{50} curves and calculation of IC_{50} values was performed with *GraphPad Prism 5.01*.

***In Vivo* Experiments.** For the *in vivo* testing of E-[c(RGDfK)$_2$], E-[c(RGDfK)$_2$]-DOXO-1, E-[c(RGDfK)$_2$]-DOXO-2, and c(RADfK)-DOXO-2 in comparison with doxorubicin female NMRI: nu/nu mice (M&B A/S, Ry, Denmark) were used. The mice were held in laminar flow shelves under sterile and standardized environmental conditions (25 ± 2 °C room temperature, 50 ± 10% relative humidity, 12 h light−dark rhythm). They received autoclaved food and bedding (ssniff, Soest, FRG) and acidified (pH 4.0) drinking water *ad libitum*. All animal experiments were performed under the auspices of the German Animal Protection Law. Orientating toxicity study with E-[c(RGDfK)$_2$]-DOXO-2 was carried out at doses of 8, 16, and 24 mg/kg doxorubicin equivalents. E-[c(RGDfK)$_2$]-DOXO-2 was dissolved in glucose phosphate buffer (10 mM

Scheme 1. Preparation of E⁻[c(RGDfK)$_2$]-DOXO^{-1} and E⁻[c(RGDfK)$_2$]-DOXO^{-2}

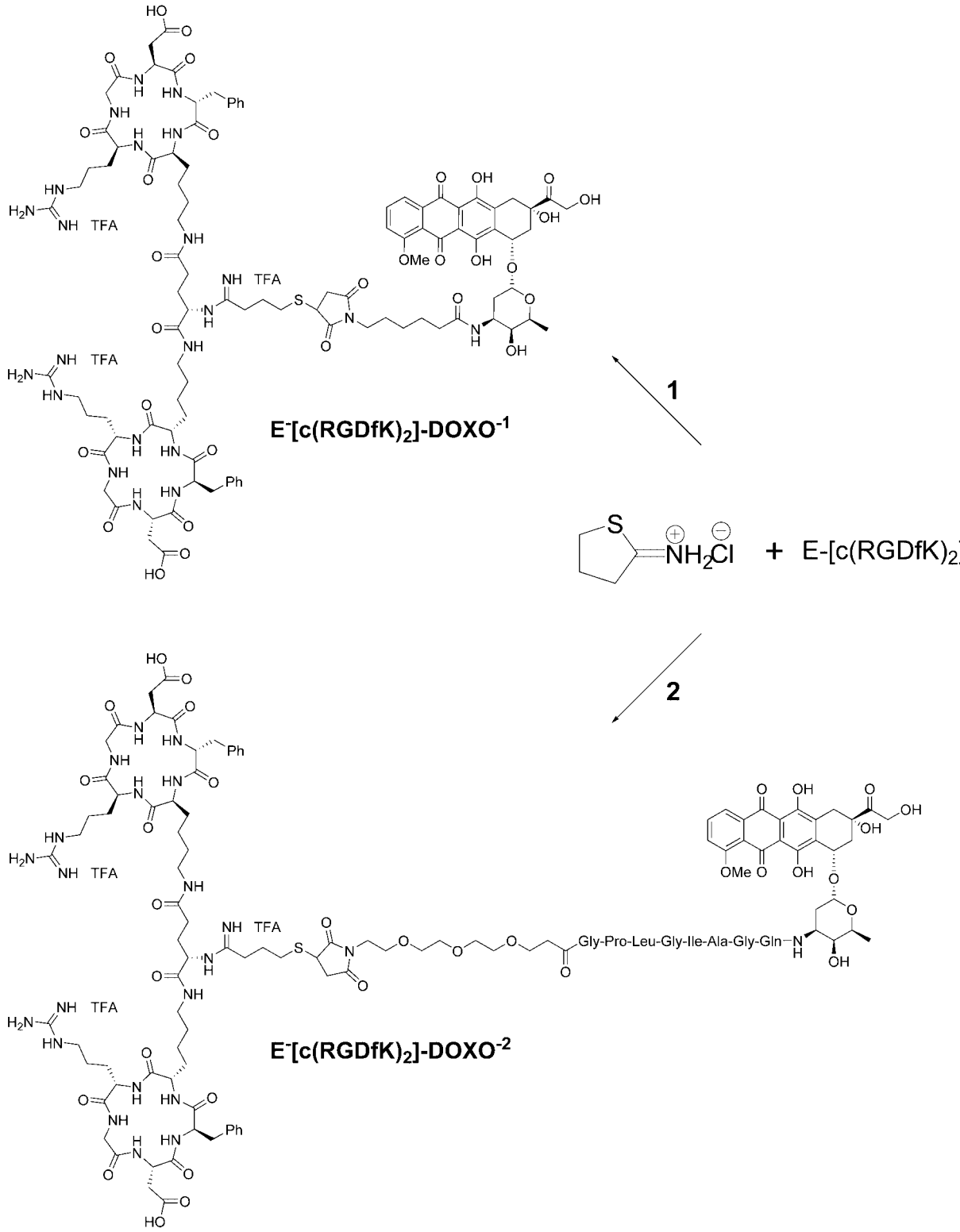

sodium phosphate, 5% D-(+)-glucose, pH 5.8) at a concentration of 3 mM and administered intravenously (i.v.) in a weekly schedule. For experiments in tumor-bearing animals, 10^7 cells of human ovarian cancer cells OVCAR-3 from *in vitro* culture were transplanted subcutaneously (s.c.) into the flank region of anaesthetized (40 mg/kg i.p. Radenarkon, Asta Medica, Frankfurt, FRG) mice on day zero. Mice were randomly distributed to the experimental groups (8 mice for control, 6 mice each for the treatment groups). When the tumors were grown to a palpable size, treatment was initiated (Figure 8). Mice were treated intravenously at day 10, 17, and 24 with glucose phosphate buffer (10 mM sodium phosphate, 5% D-(+)-glucose, pH 5.8), E-[c(RGDfK)$_2$], dissolved in glucose phosphate buffer (10 mM sodium phosphate, 5% D-(+)-glucose, pH 5.8) at a concentration of 7 mM (3 × 54.5 mg/kg), doxorubicin (2 × 8 mg/kg), E-[c(RGDfK)$_2$]-DOXO-1, dissolved in glucose phosphate buffer (10 mM sodium phosphate, 5% D-(+)-glucose, pH 5.8) at a concentration of 4 mM (3 × 24 mg/kg), E-[c(RGDfK)$_2$]-DOXO-2, dissolved in glucose phosphate buffer (10 mM sodium phosphate, 5% D-(+)-glucose, pH 5.8) at a concentration of 3

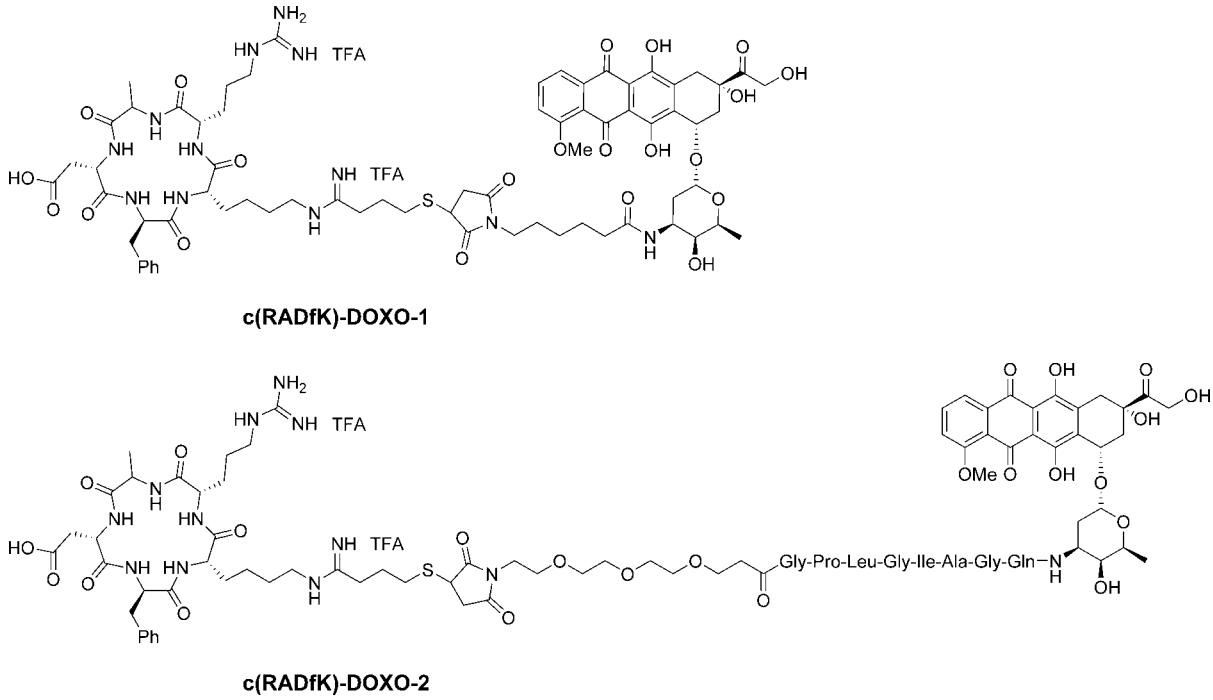

Figure 3. Structure of c(RADfK)-DOXO-1 and c(RADfK)-DOXO-2.

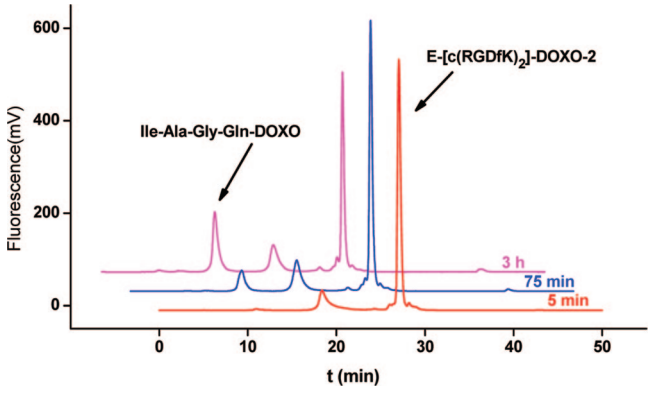

Figure 4. Chromatograms of incubation studies of a 200 μM solution of E-[c(RGDfK)$_2$]-DOXO-2 with 58.8 mU activated MMP-2 at 37 °C. Chromatographic conditions: see Experimental Procedures.

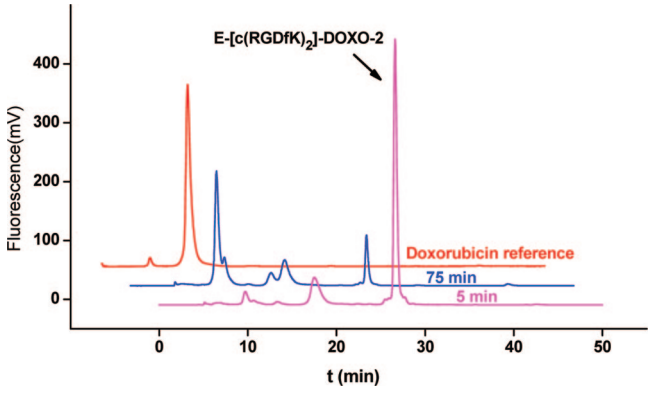

Figure 5. Chromatograms of incubation studies of a 100 μM solution of E-[c(RGDfK)$_2$]-DOXO-2 with OVCAR-3 tumor homogenates at 37 °C. Chromatographic conditions: see Experimental Procedures.

mM (2 × 8 mg/kg, 3 × 24 mg/kg), or c(RADfK)-DOXO-2, dissolved in glucose phosphate buffer (10 mM sodium phosphate, 5% D-(+)-glucose, pH 5.8) at a concentration of 6 mM (3 × 24 mg/kg) freshly dissolved in glucose phosphate buffer.

Tumor size was measured twice weekly with a caliper-like instrument in two dimensions. Individual tumor volumes (V) were calculated by the formula $V = (\text{length} + [\text{width}]^2)/2$ and related to the values on the first day of treatment (relative tumor volume, RTV). Statistical analysis was performed with the U-test (Mann and Whitney) with $p < 0.05$. The body weights of mice were determined every 3 to 4 days.

RESULTS

Chemistry. A series of acid-sensitive and enzymatically cleavable maleimide drug derivatives have been developed in our group that react specifically and selectively with thiol groups, e.g., with the cysteine-34 position of circulating albumin (*18, 22–28*). Maleimide doxorubicin derivatives were therefore an obvious choice for developing conjugates with E-[c(RGDfK)$_2$]. The precursor **1** for the stable conjugates was obtained by reaction of doxorubicin hydrochloride and 6-maleimidohexanoic acid *N*-hydroxysuccinimide ester. By introducing a thiol group with 2-iminothiolane (Traut's reagent) at the α-amino position of the glutamic acid moiety of E-[c(RGDfK)$_2$], we discovered that doxorubicin conjugates with **1** and **2** could be conveniently synthesized in a one-pot reaction of 2-iminothiolane, E-[c(RGDfK)$_2$], and the respective 6-maleimide derivate **1** or **2**. Subsequently, the resulting conjugates were isolated by preparative HPLC, thus obtaining E-[c(RGDfK)$_2$]-DOXO-1 and E-[c(RGDfK)$_2$]-DOXO-2 (Scheme 1). The analogously constructed doxorubicin conjugates with the control peptide c(RADfK), c(RADfK)-DOXO-1, and c(RADfK)-DOXO-2 were obtained in the same manner (Figure 3 and Experimental Procedures section). The conjugates showed good water solubility in glucose phosphate buffer (10 mM sodium phosphate, 5% D-(+)-glucose, pH 5.8) of ~10 mg/mL for E-[c(RGDfK)$_2$]-DOXO-1, c(RADfK)-DOXO-1, and c(RADfK)-DOXO-2 and ~20 mg/mL for E-[c(RGDfK)$_2$]-DOXO-2. The conjugates were characterized by analytical HPLC and MALDI TOF (see Experimental Procedures section).

Stability and Cleavage Properties of RGD Doxorubicin Conjugates. Stability of E-[c(RGDfK)$_2$]-DOXO-2 was studied at pH 7.0 (FPLC buffer; 150 mM NaCl, 4 mM Na_2HPO_4) at room temperature. Chromatograms were recorded over a period of 24 h showing minor decomposition of 17% (data not shown).

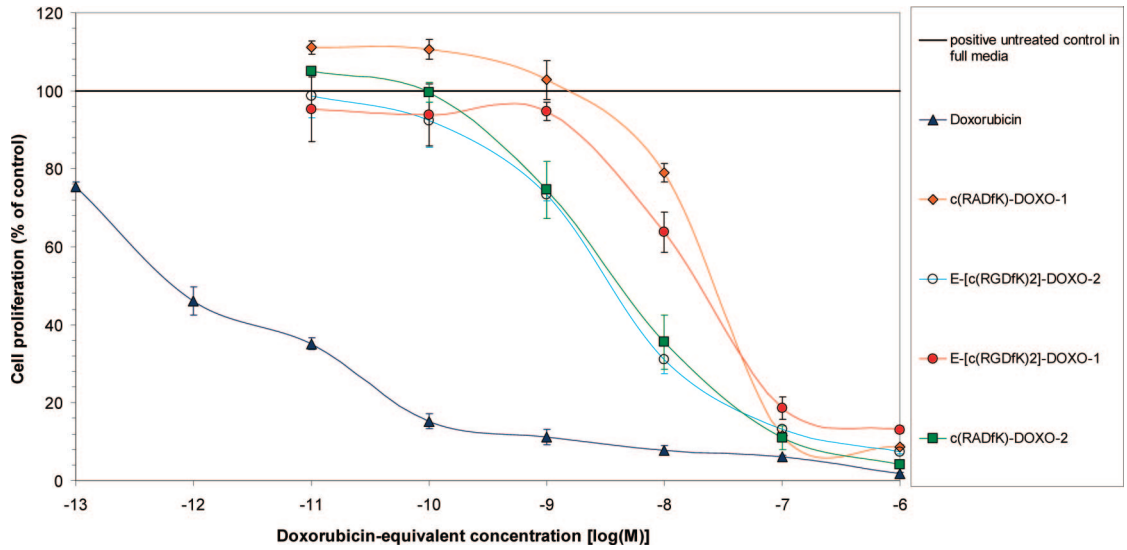

Figure 6. HUVEC proliferation assay treated with free doxorubicin (closed triangles, mean IC_{50} = 700 fM) and doxorubicin derivatives: E-[c(RGDfK)$_2$]-Doxo-1 (closed circles, mean IC_{50} = 20 nM), E-[c(RGDfK)$_2$]-Doxo-2 (open circles, mean IC_{50} = 3.5 nM), c(RADfK)-Doxo-1 (closed diamond, mean IC_{50} = 28 nM), and c(RADfK)-Doxo-2 (closed squares, mean IC_{50} = 4.2 nM). Solid line represents positive control of HUVEC proliferation in the presence of growth factors. Data represents mean ± standard deviation of the mean. HUVEC proliferation was significantly inhibited by free doxorubicin, while it was inhibited to a lesser extent by doxorubicin derivatives.

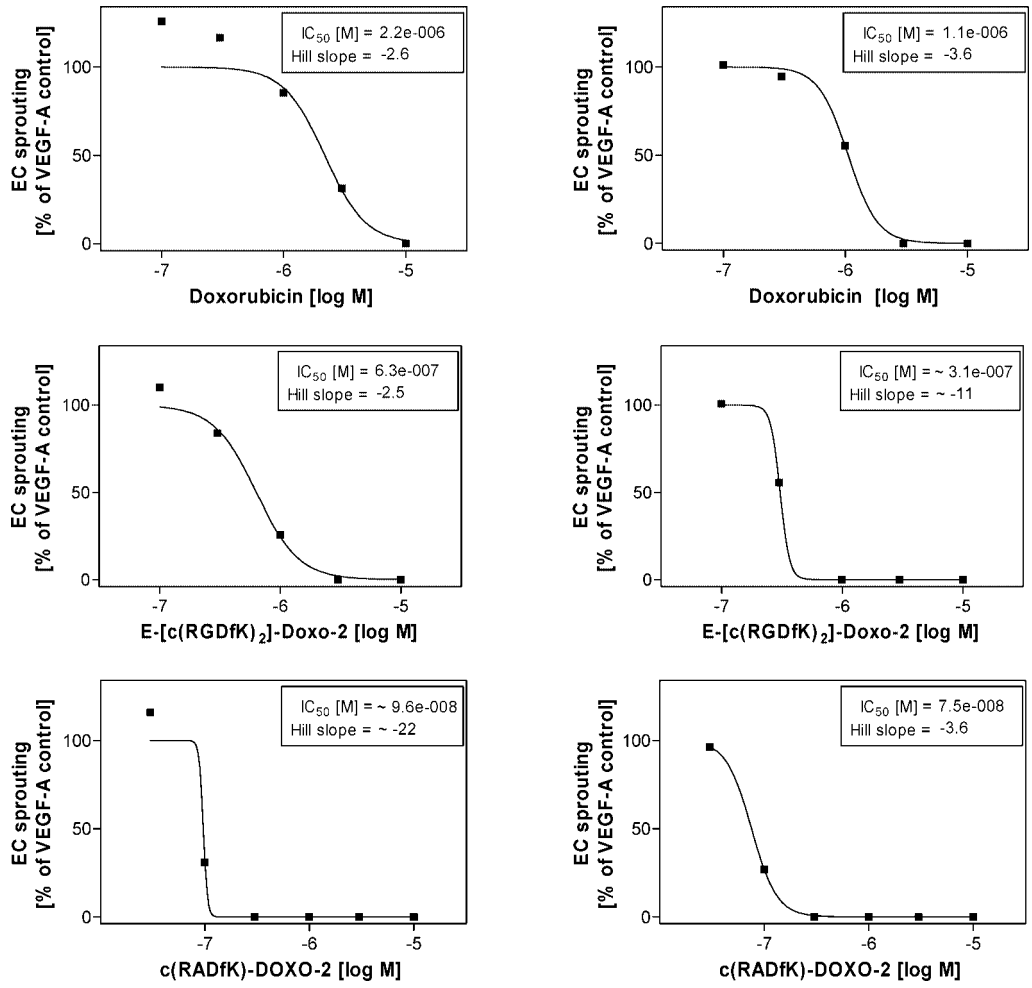

Figure 7. 3D spheroid-based angiogenesis assay. HUVEC spheroids were embedded in a 3D collagen gel, stimulated with VEGF-A [25 ng/mL], and treated for 24 h with different concentrations of doxorubicin, E-[c(RGDfK)$_2$]-DOXO-2, and c(RADfK)-DOXO-2 (in [log *M*], as indicated). The cumulative sprout length of 10 randomly selected spheroids per data point was analyzed and the relative inhibition by the test compounds determined. Two independent experiments were performed. Fitting of IC_{50} curves and calculation of IC_{50} values was performed with *GraphPad Prism 5.01*. HUVEC sprouting was inhibited approximately 3.5-fold more strongly with E-[c(RGDfK)$_2$]-DOXO-2 [mean IC_{50} = 470 nM] and approximately 20-fold stronger with c(RADfK)-DOXO-2 [mean IC_{50} = 86 nM] compared to doxorubicin [mean IC_{50} = 1700 nM].

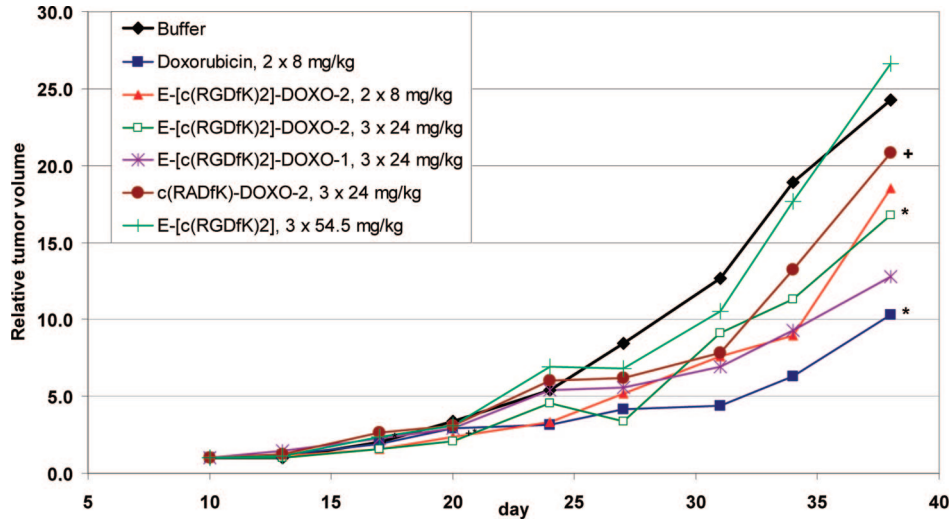

Figure 8. Curves depicting tumor growth inhibition of subcutaneously OVCAR-3 xenografts under therapy with RGD- and RAD-doxorubicin derivatives, doxorubicin, and E-[c(RGDfK)$_2$]; * significant to control; + significant to doxorubicin $p < 0.05$.

Table 1. Dose Schedule, Mortality, Body Weight Change, and Antitumor Activity of RGD- and RAD-Doxorubicin Derivatives, Doxorubicin, and E-[c(RGDfK)$_2$] against Human Ovarian Cancer Xenografts (OVCAR-3) *in Vivo*

substance	nu/nu mice	treatment (d)	dose (mg/kg/inj.)	toxic deaths (d)	BWC (%) d 10−17	optimum T/C (%) [at day]
5% Glucose-P-Buffer	8	10, 17, 24			−2	
Doxorubicin	6	10, 17	8	0	−2	33 [34][a]
E-[c(RGDfK)$_2$]-DOXO-2	6	10, 17	8	0	−3	47 [34]
E-[c(RGDfK)$_2$]-DOXO-2	6	10, 17, 24	24	1 (25)	−2	40 [27][a]
c(RADfK)-DOXO-2	6	10, 17, 24	24	3 (18, 18, 25)	−2	49 [34]
E-[c(RGDfK)$_2$]-DOXO-1	6	10, 17, 24	24	3 (18, 25, 25)	−1	70 [34][b]
E-[c(RGDfK)$_2$]	6	10, 17, 24	54, 5	0	0	80 [27]

[a] Significant to control. [b] Significant to doxorubicin $p < 0.05$.

Subsequent cleavage studies of E-[c(RGDfK)$_2$]-DOXO-2 were carried out following a modified method of Mansour et al. (*18*). The octapeptide Gly-Pro-Leu-Gly-Ile-Ala-Gly-Gln in **2** is specifically cleaved by MMP-2 and MMP-9 releasing the doxorubicin-tetrapeptide Ile-Ala-Gly-Gln-DOXO as previously shown (*18, 29*). Incubation studies of E-[c(RGDfK)$_2$]-DOXO-2 with activated MMP-2 showed a major peak at 27 min for E-[c(RGDfK)$_2$]-DOXO-2 min in the HPLC chromatogram after 5 min incubation time which decreased with time and an unidentified peak at 18 min (Figure 4). Furthermore, a peak at 13 min was observed which increased during 3 h and which we assigned as Ile-Ala-Gly-Gln-DOXO by comparison with our data from refs (*18, 29*). In OVCAR-3 tumor homogenates, the major cleavage product was doxorubicin after 75 min incubation (Figure 5). Identification of doxorubicin as the cleavage product was verified with a doxorubicin standard and spiking with doxorubicin in the cleavage experiment. In contrast, no release of doxorubicin was observed for E-[c(RGDfK)$_2$]-DOXO-1 in OVCAR-3 tumor homogenates (data not shown).

***In Vitro* Activity.** *Endothelial Cell Proliferation and Sprouting Is Inhibited by Doxorubicin-Containing RGD Peptides.* The effect of doxorubicin, and the doxorubicin derivatives E-[c(RGDfK)$_2$]-DOXO-1, E-[c(RGDfK)$_2$]-DOXO-2, c(RADfK)-DOXO-1, and c(RADfK)-DOXO-2 on endothelial cells was tested in two independent assays. First, the ability of doxorubicin derivatives to inhibit HUVEC proliferation was assessed using a standard 72 h proliferation assay. Free doxorubicin inhibited HUVEC proliferation more efficiently than the four peptide-containing doxorubicin derivatives, demonstrating an IC_{50} value of 700 fM compared to 20 nM for E-[c(RGDfK)$_2$]-DOXO-1, 3 nM for E-[c(RGDfK)$_2$]-DOXO-2, 30 nM for c(RADfK)-DOXO-1, and 5 nM for c(RADfK)-DOXO-2 (Figure 6). The E-[c(RGDfK)$_2$] peptide inhibited HUVEC proliferation by itself but only at high concentrations of 100−1000 nM. c(RADfK) peptide showed no effect even at those high concentrations (data not shown).

In a second assay, HUVEC spheroids were embedded in a 3D collagen gel, stimulated with VEGF-A, and treated for 24 h with different concentrations of doxorubicin, E-[c(RGDfK)$_2$]-DOXO-2, and c(RADfK)-DOXO-2 (in [log *M*], as indicated). As shown in Figure 7, HUVEC sprouting was inhibited ~3.5-fold stronger with E-[c(RGDfK)$_2$]-DOXO-2 [mean IC_{50} = 470 nM] and ~20-fold stronger with c(RADfK)-DOXO-2 [mean IC_{50} = 86 nM] compared to doxorubicin [mean IC_{50} = 1700 nM]. In contrast, the free peptides E-[c(RGDfK)$_2$] and c(RADfK) as well as the stable doxorubicin amide derivatives E-[c(RGDfK)$_2$]-DOXO-1 and c(RADfK)-DOXO-1 showed no activity at the highest concentration of ~10 000 nM (data not shown).

***In Vivo* Activity.** Subsequently, the *in vivo* antitumor efficacy of E-[c(RGDfK)$_2$], doxorubicin, and the doxorubicin derivatives E-[c(RGDfK)$_2$]-DOXO-1, E-[c(RGDfK)$_2$]-DOXO-2, and c(RADfK)-DOXO-2 was evaluated in xenografted nu/nu mice (human ovarian carcinoma OVCAR-3), this model being chosen because Janssen et al. showed a high uptake of radiolabeled E-[c(RGDfK)$_2$] of up to 7.5% ID/g in subcutaneously growing OVCAR-3 tumors (*11*).

Based on an orientating toxicity study with E-[c(RGDfK)$_2$]-DOXO-2 that showed a maximum tolerated dose (MTD) of 24 mg/kg doxorubicin equivalents, the following doses were chosen: doxorubicin (2 × 8 mg/kg), E-[c(RGDfK)$_2$]-DOXO-1 (3 × 24 mg/kg doxorubicin equivalents), E-[c(RGDfK)$_2$]-DOXO-2 (2 × 8 mg/kg, and 3 × 24 mg/kg doxorubicin equivalents), c(RADfK)-DOXO-2 (3 × 24 mg/kg doxorubicin equivalents), and E-[c(RGDfK)$_2$] (3 × 54.5 mg/kg, corresponding to the amount present in 3 × 24 mg/kg E-[c(RGDfK)$_2$]-DOXO-2) (Table 1). The results of the xenograft experiment are summarized in Table 1 and Figure 8. Treatment with

doxorubicin resulted in a moderate, but statistically significant, antitumor effect at its optimal dose in nu/nu mice models of 2 × 8 mg/kg (T/C max. 33%). In contrast, the free peptide E-[c(RGDfK)$_2$] and the stable amide derivative E-[c(RGDfK)$_2$]-DOXO-1 were inactive, with the latter also being toxic with a mortality of 50%. The prodrug E-[c(RGDfK)$_2$]-DOXO-2 at 2 × 8 mg/kg and 3 × 24 mg/kg showed a very moderate inhibition of tumor growth, which was statistically significant versus control only for the high-dose group. One animal died in this group. The prodrug c(RADfK)-DOXO-2 with the nonintegrin $\alpha_v\beta_3$ binding control peptide showed a high mortality at 3 × 24 m/kg and doxorubicin equivalents (50%). The remaining three animals showed a slightly better antitumor efficacy than the five animals treated with E-[c(RGDfK)$_2$]-DOXO-2, although this antitumor effect was not statistically significant compared to the control.

DISCUSSION

Integrins, especially integrin $\alpha_v\beta_3$, have served as an attractive target for designing drug delivery systems ranging from RGD-based liposomes (*30, 31*), protein (*32*) or polymer conjugates (*33*), and nanoparticles (*34*).

A key result in this field was the discovery of the divalent RGD-4C peptide using a phage-display library (*7*). Subsequent development and evaluation of doxorubicin conjugates with RGD-4C have, however, not resulted in a clear picture of the structural requirements that a doxorubicin RGD conjugate should have for effective *in vivo* vascular targeting. In this work, we therefore developed doxorubicin conjugates with the divalent RGD peptide, E-[c(RGDfK)$_2$], which is more stable than RGD-4C and meanwhile commercially available. Synthesis of the conjugates was achieved by thiolating the free amino group of E-[c(RGDfK)$_2$] or of the control peptide c(RADfK) and reacting the stable maleimide doxorubicin derivative **1** or a MMP-2 cleavable doxorubicin derivative **2** with the introduced thiol group yielding E-[c(RGDfK)$_2$]-DOXO-1 and E-[c(RGDfK)$_2$]-DOXO-2, c(RADfK)-DOXO-1, and c(RADfK)-DOXO-2. E-[c(RGDfK)$_2$]-DOXO-2 was effectively cleaved by MMP-2 and in OVCAR-3 tumor homogenates releasing a doxorubicin-tetrapeptide or doxorubicin as the final cleavage product demonstrating a clear prodrug nature for **2**. In contrast, E-[c(RGDfK)$_2$]-DOXO-1 was stable in OVCAR-3 tumor homogenates. In a cytotoxicity assay against HUVEC, E-[c(RGDfK)$_2$]-DOXO-1 and E-[c(RGDfK)$_2$]-DOXO-2 as well as their c(RADfK) analogues showed cytotoxicity in the low nanomolar range, the cytotoxicity being more dependent on the cleavability than the nature of the RGD peptide (Figure 6). Surprisingly, in a HUVEC sprouting assay the doxorubicin prodrug with the control peptide, c(RADfK)-DOXO-2, was more active than E-[c(RGDfK)$_2$]-DOXO-2 (Figure 7), whereas E-[c(RGDfK)$_2$]-DOXO-1 and c(RADfK)-DOXO-1 were inactive, indicating that interactions with other membrane-associated targets besides integrin $\alpha_v\beta_3$ could be important.

In vivo, neither doxorubicin conjugates with E-[c(RGDfK)$_2$] nor c(RADfK) showed convincing antitumor efficacy. This result is disappointing considering that much larger doses (3 × 24 mg/kg doxorubicin equivalents) than the MTD of doxorubicin in nu/nu mice models (2 × 8 mg/kg) were administered. In contrast, the albumin-binding prodrug **2** has shown superior efficacy compared to doxorubicin in a melanoma xenograft model (*18*). There are a number of reasons that could explain the lack of efficacy of our new conjugates: (1) The targeting potential of the new conjugates is insufficient, although this explanation does not seem likely considering the convincing evidence of tumor uptake that Janssen et al. has collected with radiolabeled E-[c(RGDfK)$_2$] in the OVCAR-3 xenograft model (*12*), the same that model that we used in our studies. (2) After binding of E-[c(RGDfK)$_2$] to endothelial cells, the doxorubicin conjugates are taken up rapidly by endocytosis that would prevent the cleavage of E-[c(RGDfK)$_2$]-DOXO-2 by the extracellular proteases MMP-2 and MMP-9. There are data supporting an internalization of RGD peptides in integrin $\alpha_v\beta_3$ expressing and nonexpressing melanoma cells by an integrin-independent fluid-phase endocytosis pathway (*35*). Our own investigations do not support cleavage of the MMP-2 cleavable octapeptide when tumor homogenates at pH 5.0 are used that preserve activity of lysosomal proteases (*36*). (3) The potency of doxorubicin is not sufficient for receptor targeting of integrin $\alpha_v\beta_3$. The interaction of E-[c(RGDfK)$_2$]-DOXO-2 with integrin might be limited due to an insufficient receptor density on endothelial cells or a rapid clearance of E-[c(RGDfK)$_2$]-DOXO-2 leading to low amounts of doxorubicin reaching endothelial cells. Thus, targeting of integrin $\alpha_v\beta_3$-expressing cells could be improved by using highly potent cytotoxic drugs in line with the clear trend of using such agents for the development of drug antibody conjugates that are designed for receptor or antigen targeting (*37, 38*).

In our current work, we are addressing the nature of the enzymatically cleavable linker as well as the drug component on RGD-based drug conjugates.

ACKNOWLEDGMENT

The support of the Deutsche Forschungsgemeinschaft (DFG) is gratefully acknowledged. This study was supported by a Postdoctoral Fellowship (HMS) from the Israel Cancer Research Fund. This research was supported by The Israel Science Foundation (grant No. 1300/06) and the Igal Alon Fellowship (RSF).

Supporting Information Available: MALDI-TOF and ESI-TOF spectra of compound **1**, E-[c(RGDfK)$_2$]-DOXO-1, E-[c(RGDfK)$_2$]-DOXO-2, c(RADfK)-DOXO-1, and c(RADfK)-DOXO-2.This material is available free of charge via the Internet at http://pubs.acs.org.

LITERATURE CITED

(1) Maier, J. A., Delia, D., Thorpe, P. E., and Gasparini, G. (1997) In vitro inhibition of endothelial cell growth by the antiangiogenic drug AGM-1470 (TNP-470) and the anti-endoglin antibody TEC-11. *Anticancer Drugs 8*, 238–244.

(2) Neri, D., and Bicknell, R. (2005) Tumour vascular targeting. *Nat. Rev. Cancer 5*, 436–446.

(3) Ruoslahti, E. (2002) Drug targeting to specific vascular sites. *Drug Discovery Today 7*, 1138–1143.

(4) Satchi-Fainaro, R. (2002) Targeting tumor vasculature: reality or a dream? *J. Drug Targeting 10*, 529–533.

(5) Temming, K., Schiffelers, R. M., Molema, G., and Kok, R. J. (2005) RGD-based strategies for selective delivery of therapeutics and imaging agents to the tumour vasculature. *Drug Resist. Update 8*, 381–402.

(6) Pasqualini, R., Koivunen, E., and Ruoslahti, E. (1997) Alpha v integrins as receptors for tumor targeting by circulating ligands. *Nat. Biotechnol. 15*, 542–546.

(7) Arap, W., Pasqualini, R., and Ruoslahti, E. (1998) Cancer treatment by targeted drug delivery to tumor vasculature in a mouse model. *Science 279*, 377–380.

(8) Kim, J. W., and Lee, H. S. (2004) Tumor targeting by doxorubicin-RGD-4C peptide conjugate in an orthotopic mouse hepatoma model. *Int. J. Mol. Med. 14*, 529–535.

(9) de Groot, F. M., Broxterman, H. J., Adams, H. P., van Vliet, A., Tesser, G. I., Elderkamp, Y. W., Schraa, A. J., Kok, R. J., Molema, G., Pinedo, H. M., and Scheeren, H. W. (2002) Design, synthesis, and biological evaluation of a dual tumor-specific motive containing integrin-targeted plasmin-cleavable doxorubicin prodrug. *Mol. Cancer Ther. 1*, 901–911.

(10) Haubner, H., Gratias, R., Diefenbach, B., Goodman, S. L., Jonczyk, A., and Kessler, H. (1996) Structural and functional aspects of RGD-containing cyclic pentapeptides as highly potent and selective integrin alpha(v)beta(3) antagonists. *J. Am. Chem. Soc. 118*, 7461–7472.

(11) Janssen, M., Oyen, W. J., Massuger, L. F., Frielink, C., Dijkgraaf, I., Edwards, D. S., Radjopadhye, M., Corstens, F. H., and Boerman, O. C. (2002) Comparison of a monomeric and dimeric radiolabeled RGD-peptide for tumor targeting. *Cancer Biother. Radiopharm. 17*, 641–646.

(12) Janssen, M. L., Oyen, W. J., Dijkgraaf, I., Massuger, L. F., Frielink, C., Edwards, D. S., Rajopadhye, M., Boonstra, H., Corstens, F. H., and Boerman, O. C. (2002) Tumor targeting with radiolabeled alpha(v)beta(3) integrin binding peptides in a nude mouse model. *Cancer Res. 62*, 6146–6151.

(13) Janssen, M., Frielink, C., Dijkgraaf, I., Oyen, W., Edwards, D. S., Liu, S., Rajopadhye, M., Massuger, L., Corstens, F., and Boerman, O. (2004) Improved tumor targeting of radiolabeled RGD peptides using rapid dose fractionation. *Cancer Biother. Radiopharm. 19*, 399–404.

(14) Burkhart, D. J., Kalet, B. T., Coleman, M. P., Post, G. C., and Koch, T. H. (2004) Doxorubicin-formaldehyde conjugates targeting alphavbeta3 integrin. *Mol. Cancer Ther. 3*, 1593–1604.

(15) Deryugina, E. I., Ratnikov, B., Monosov, E., Postnova, T. I., DiScipio, R., Smith, J. W., and Strongin, A. Y. (2001) MT1-MMP initiates activation of pro-MMP-2 and integrin alphavbeta3 promotes maturation of MMP-2 in breast carcinoma cells. *Exp. Cell Res. 263*, 209–223.

(16) Deryugina, E. I., and Quigley, J. P. (2006) Matrix metalloproteinases and tumor metastasis. *Cancer Metastasis Rev. 25*, 9–34.

(17) Rolli, M., Fransvea, E., Pilch, J., Saven, A., and Felding-Habermann, B. (2003) Activated integrin alphavbeta3 cooperates with metalloproteinase MMP-9 in regulating migration of metastatic breast cancer cells. *Proc. Natl. Acad. Sci. U.S.A. 100*, 9482–9487.

(18) Mansour, A. M., Drevs, J., Esser, N., Hamada, F. M., Badary, O. A., Unger, C., Fichtner, I., and Kratz, F. (2003) A new approach for the treatment of malignant melanoma: enhanced antitumor efficacy of an albumin-binding doxorubicin prodrug that is cleaved by matrix metalloproteinase 2. *Cancer Res. 63*, 4062–4066.

(19) Kussmann, M., Lässing, U., Stürmer, C. A., Przybylski, M., and Roepstorff, P. (1997) Matrix-assisted laser desorption/ionization mass spectrometric peptide mapping of the neural cell adhesion protein neurolin purified by sodium dodecyl sulfate polyacrylamide gel electrophoresis or acidic precipitation. *J. Mass Spectrom. 32*, 483–493.

(20) Korff, T., and Augustin, H. G. (1998) Integration of endothelial cells in multicellular spheroids prevents apoptosis and induces differentiation. *J. Cell Biol. 143*, 1341–1352.

(21) Korff, T., and Augustin, H. G. (1999) Tensional forces in fibrillar extracellular matrices control directional capillary sprouting. *J. Cell Sci. 112* (Pt 19), 3249–3258.

(22) Schmid, B., Chung, D. E., Warnecke, A., Fichtner, I., and Kratz, F. (2007) Albumin-binding prodrugs of camptothecin and doxorubicin with an Ala-Leu-Ala-Leu-linker that are cleaved by cathepsin B: synthesis and antitumor efficacy. *Bioconjugate Chem. 18*, 702–16.

(23) Schmid, B., Warnecke, A., Fichtner, I., Jung, M., and Kratz, F. (2007) Development of albumin-binding camptothecin prodrugs using a Peptide positional scanning library. *Bioconjugate Chem. 18*, 1786–99.

(24) Kratz, F., Warnecke, A., Scheuermann, K., Stockmar, C., Schwab, J., Lazar, P., Drückes, P., Esser, N., Drevs, J., Rognan, D., Bissantz, C., Hinderling, C., Folkers, G., Fichtner, I., and Unger, C. (2002) Probing the cysteine-34 position of endogenous serum albumin with thiol-binding doxorubicin derivatives: improved efficacy of an acid-sensitive doxorubicin derivative with specific albumin-binding properties compared to that of the parent compound. *J. Med. Chem. 45*, 5523–5533.

(25) Kratz, F. (2007) DOXO-EMCH (INNO-206): the first albumin-binding prodrug of doxorubicin to enter clinical trials. *Expert Opin. Invest. Drugs 16*, 855–866.

(26) Kratz, F., Mansour, A., Soltau, J., Warnecke, A., Fichtner, I., Unger, C., and Drevs, J. (2005) Development of albumin-binding doxorubicin prodrugs that are cleaved by prostate-specific antigen. *Arch. Pharm. (Weinheim) 338*, 462–472.

(27) Warnecke, A., Fichtner, I., Garmann, D., Jaehde, U., and Kratz, F. (2004) Synthesis and biological activity of water-soluble maleimide derivatives of the anticancer drug carboplatin designed as albumin-binding prodrugs. *Bioconjugate Chem. 15*, 1349–1359.

(28) Warnecke, A., and Kratz, F. (2003) Maleimide-oligo(ethylene glycol) derivatives of camptothecin as albumin-binding prodrugs: synthesis and antitumor efficacy. *Bioconjugate Chem. 14*, 377–387.

(29) Kratz, F., Drevs, J., Bing, G., Stockmar, C., Scheuermann, K., Lazar, P., and Unger, C. (2001) Development and in vitro efficacy of novel MMP2 and MMP9 specific doxorubicin albumin conjugates. *Bioorg. Med. Chem. Lett. 11*, 2001–2006.

(30) Schiffelers, R. M., Molema, G., ten Hagen, T. L., Janssen, A. P., Schraa, A. J., Kok, R. J., Koning, G. A., and Storm, G. (2002) Ligand-targeted liposomes directed against pathological vasculature. *J. Liposome Res. 12*, 129–135.

(31) Xiong, X. B., Huang, Y., Lu, W. L., Zhang, X., Zhang, H., Nagai, T., and Zhang, Q. (2005) Enhanced intracellular delivery and improved antitumor efficacy of doxorubicin by sterically stabilized liposomes modified with a synthetic RGD mimetic. *J. Controlled Release 107*, 262–275.

(32) Temming, K., Meyer, D. L., Zabinski, R., Senter, P. D., Poelstra, K., Molema, G., and Kok, R. J. (2007) Improved efficacy of alphavbeta3-targeted albumin conjugates by conjugation of a novel auristatin derivative. *Mol. Pharm. 4*, 686–694.

(33) Mitra, A., Coleman, T., Borgman, M., Nan, A., Ghandehari, H., and Line, B. R. (2006) Polymeric conjugates of mono- and bi-cyclic alphaVbeta3 binding peptides for tumor targeting. *J. Controlled Release 114*, 175–183.

(34) Xie, J., Shen, Z., Li, K. C., and Danthi, N. (2007) Tumor angiogenic endothelial cell targeting by a novel integrin-targeted nanoparticle. *J. Nanomedicine 2*, 479–485.

(35) Castel, S., Pagan, R., Mitjans, F., Piulats, J., Goodman, S., Jonczyk, A., Huber, F., Vilaró, S., and Reina, M. (2001) RGD peptides and monoclonal antibodies, antagonists of alpha(v)-integrin, enter the cells by independent endocytic pathways. *Lab. Invest. 81*, 1615–1626.

(36) Werle, B., Ebert, W., Klein, W., and Spiess, E. (1994) Cathepsin B in tumors, normal tissue and isolated cells from the human lung. *Anticancer Res. 14*, 1169–1176.

(37) Kratz, F., Müller, I. A., Ryppa, C., and Warnecke, A. (2008) Prodrug strategies in anticancer chemotherapy. *ChemMedChem 3*, 20–53.

(38) Wu, A. W., and Senter, P. D. (2005) Arming antibodies. *Nat. Biotechnol. 23*, 1137–1146.

BC800117R